

DEBONDING OF A MODEL SOFT ADHESIVE: FROM A VISCOUS LIQUID TO AN ELASTIC SOLID

Julia Nase*, Anke Lindner*, Costantino Creton**

* PMMH - ESPCI, 75005 Paris, France, nase@pmmh.espci.fr, lindner@ccr.jussieu.fr

** PPMD - ESPCI, 75005 Paris, France, Costantino.Creton@espci.fr

Introduction

Good adhesives show viscoelastic properties that allow on the one hand having a good molecular contact with the substrate and on the other hand a strong resistance to a certain stress level during debonding. Studying the fine balance between the liquid and the solid character that determines the debonding process is crucial for a better understanding of the adhesive's performance.

Materials and Methods

To perform a systematic study of the debonding process, we need a model material system with controllable viscoelastic properties and a reproducible debonding test in a simple geometry.

We chose as a model system a weakly cross linked polymer, PDMS (Polydimethylsiloxane). We are using a commercial product, the "Sylgard 184 silicone elastomer kit" purchased at Dow Corning. It consists of a silicone oil, called the base, and a curing agent that is able to form cross links, *i.e.* chemical bonds between the polymer chains. This material is often used in its fully cured state for microfluidic applications. Without adding any curing agent, the PDMS is a Newtonian liquid. As curing agent is added, more and more cross links are formed and the material becomes viscoelastic. Adding about 10% of curing agent finally yields the fully cured elastic solid. This two component system thus represents an ideal model system that provides a reproducible and easy way to go continuously from a viscous liquid to an elastic solid.

In detail, the preparation procedure for our samples is as follows: We add a certain amount of curing agent (about 0.1g) to the base (between 5 to 10g). Then we mix thoroughly with a magnetic mixer during 10 to 15 minutes. During mixing, air bubbles are trapped in the oil. Therefore, we degas the liquid under vacuum in a desiccator at room temperature for about half an hour until all visible oxygen bubbles have disappeared.

To determine the rheological properties of the different materials, we cross link a small amount of the product directly in the rheometer and perform dynamic frequency sweep tests after curing. In that way we have access to the storage and loss moduli, G' and G'' that are measures for the material's elastic and viscous properties, respectively, as well as to the absolute value of the complex viscosity,

$$|\eta| = (G'^2 + G''^2)^{1/2} / \omega .$$

Figure 1 shows the characterization of the linear viscoelastic properties of materials with different amounts of cross

linker. The material with about 3% of cross linker is elastic, having a G' several orders of magnitude higher than G'' , whereas an amount of about 1% of cross linker leads to a product in the viscoelastic regime. Considering the complex viscosity as defined before, we find a strong decrease with frequency, see Figure 2. By analogy with the classical shear viscosity of pure liquids one can refer to these materials as shear thinning.

To perform well controlled debonding tests, we use the "probe tack" set up [1]. It mainly consists of a flat circular steel probe that can be brought into contact and debonded from a tacky adhesive sample with a controlled speed. During the test, the probe displacement and the normal force on the probe are measured. We also visualize the debonding process, *i.e.* the air penetrating into the adhesive, from above with a camera mounted on a microscope. The steel probe has a diameter D of 6mm and is made of stainless steel. It is carefully polished to assure a smooth surface and sharp edges without any irregularities.

After degassing, we prepare polymeric films on thick microscopic glass slides that are precleaned and coated with a primer to enhance the PDMS' adherence to the glass surface. To deposit PDMS films we use applicators of different thicknesses. The PDMS films are cured in the desiccator at 80°C for five hours under vacuum to remove again all oxygen bubbles that might have formed during the preparation process.

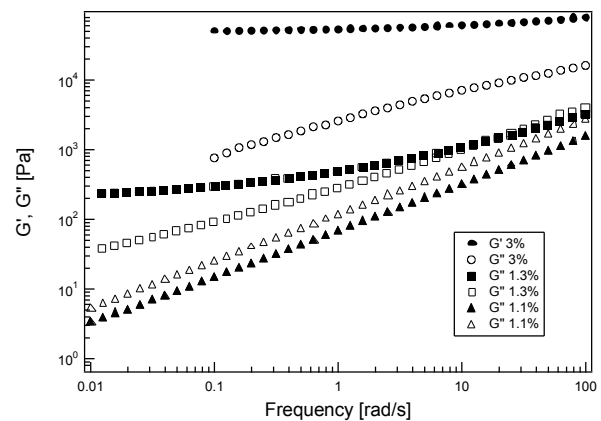


Figure 1. Changing the amount of curing agent and varying thereby the number of crosslink points results in materials with different viscoelastic properties.

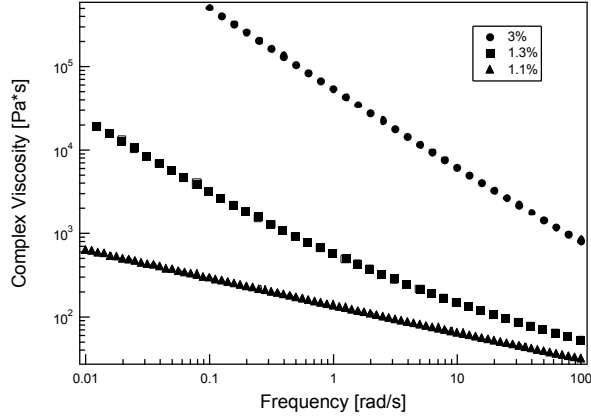


Figure 2. All materials are shear thinning with respect to the complex viscosity.

Experimental

The parameters we vary in our experiments, besides the number of cross link points and thus the adhesive's viscoelastic properties, are the initial thickness of the adhesive layer and the debonding speed. Typical thicknesses b lie between $50\mu\text{m}$ and $500\mu\text{m}$, typical debonding speeds v between $1\mu\text{m/s}$ and $200\mu\text{m/s}$.

During a typical debonding experiment, air penetrates from the edge of the adhesive layer. It can penetrate either in the adhesive's bulk, followed by a strong deformation and the subsequent formation of thin adhesive "bridges" (fibrils) between the probe and the glass slide (cohesive debonding), or at the interface between the probe surface and the polymer film, leading to a fast debonding by interfacial crack propagation (adhesive debonding). In both cases, we observe the destabilization of the initially circular debonding line by undulations and the subsequent propagation of air fingers, see Figure 3 and Figure 4. We characterize the emerging patterns by determining the finger number n at the moment the first undulations are observable and calculate a wavelength $\lambda = 2\pi R/n$.

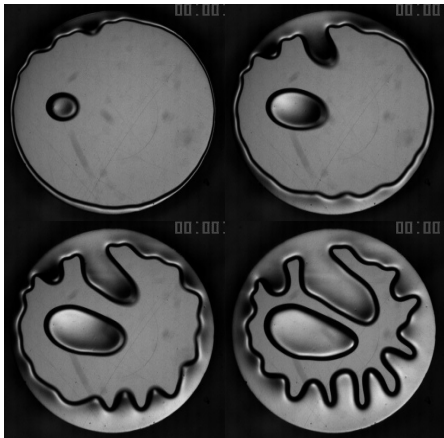


Figure 3. Formation of air fingers in the elastic case, 3%: debonding at the interface.

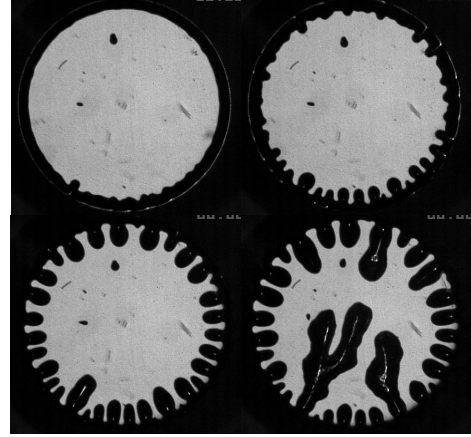


Figure 4. Formation of air fingers in the viscoelastic case, 1.2%: debonding in the bulk.

Results and Discussion

We describe and characterize here in more detail the two cases of interfacial and bulk mechanisms mentioned above. In the case of the viscoelastic regime where we find fibrillation and a cohesive debonding mechanism, the pattern formation is sensitive to both the initial film thickness and the debonding speed for a given material. The wavelength decreases with the debonding speed and increases linearly with the initial film thickness. To find the proper scaling of the wavelength λ with the thickness b , the debonding speed v and the complex viscosity $\eta(v)$, we turn to the case of a purely viscous liquid. This corresponds to the *Saffman - Taylor* or *viscous fingering* instability [2], yielding the formula

$$\lambda = \pi b / \text{Ca}^{1/2} \text{ with } \text{Ca} = U\eta / \sigma \text{ [3].}$$

$\sigma = 20\text{mN/m}$ is the surface tension, U denotes the radial velocity of the circular interface between air and adhesive. Presuming an incompressible fluid and therefore volume conservation U can be calculated as $U = Rv/2b$ for a Newtonian fluid. Note that this result is obtained by a linear stability analysis and corresponds thus to the initial destabilization of the moving interface.

To adapt this formula to our case of Non Newtonian liquids, we replace in a first step the classical viscosity by the absolute value of the complex viscosity as mentioned above. As it experiences a strong dependence on the frequency, we have to determine the correct frequency for each of our experiments. We estimate the frequency following $\omega = 2\pi U/b$.

Doing so, we find that the data for different thicknesses, debonding speeds and adhesives scale relatively well on one straight line, see Figure 5. Despite some scattering, we find good quantitative agreement with the Saffman - Taylor prediction.

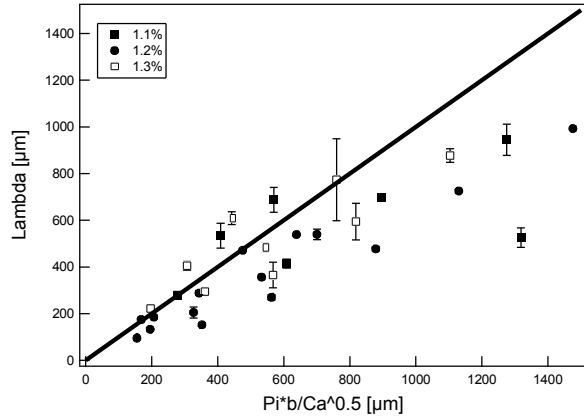


Figure 5. In the viscoelastic case, the wavelength scales linearly with the thickness and is inversely proportional to the square root of the capillary number.

In the elastic regime we do not see any dependency on the debonding speed or the storage modulus as all data fall on the same straight line. The wavelength depends only on the initial film thickness b , see Figure 6. This holds for three orders of magnitude of G^* (Figure 7).

These results for the elastic case are in agreement with theoretical predictions and with experimental observations in a slightly different geometry, see [4]. We find the relation $\lambda = 2.3*b$, compared to theoretical calculations that yield $\lambda = 3.5*b$ in reference [5].

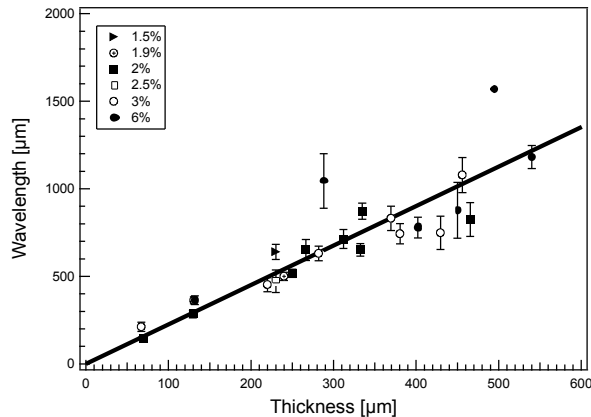


Figure 6. In the elastic case, the wavelength only scales with the thickness of the PDMS - films.

To compare the two regimes directly and to obtain information on the transition between them, we trace the reduced wavelength as a function of the complex modulus $G^* = (G'^2 + G''^2)^{1/2}$, see Figure 7. On this graph one can well distinguish the two regimes: on one hand the viscoelastic, modulus-dependent case at smaller values of G^* , and on the other hand the constant, modulus-independent elastic regime for higher values of G^* . It is however clear that G^* is not the parameter that controls the transition between the two regimes: we observe an overlap region at

values of about 3 kPa, where both interfacial and bulk mechanisms can be found.

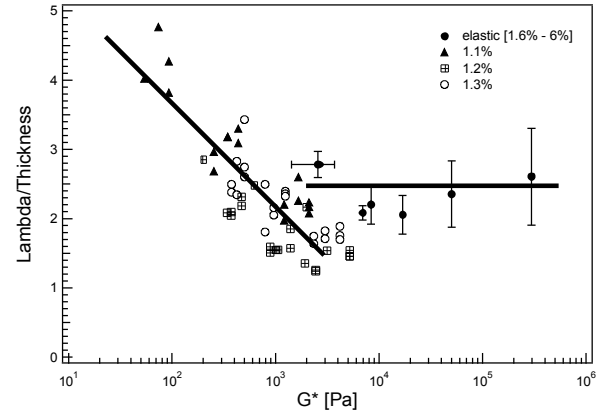


Figure 7. The viscous and elastic regime are clearly distinguishable as a function of G^* , but there is an overlap region at the transition point.

Conclusions

We perform a systematic study of the debonding process of a soft adhesive as a function of the viscoelastic properties. We established a reproducible model system that allows to go continuously from a viscous liquid to an elastic solid and characterized its rheology completely. In our experiments, we can clearly distinguish an interfacial debonding mechanism in the elastic case and a bulk mechanism in the viscoelastic case. For both regimes we find good scaling laws and a reasonable quantitative agreement with the theoretical predictions.

Further experiments will be conducted to find the right control parameter that describes the transition between the viscoelastic and the elastic regime. One approach is to take into account the probe's adhesion energy and therefore perform experiments with treated probe surfaces.

Acknowledgements

We thank Guylaine Ducouret (PPMD-ESPCI) for help with the rheological measurements and José Lanuza (PMMH-ESPCI) for help and advice concerning the experiments. We thank Arezki Boudaoud and Mokhtar Adda-Bedia (LPS-ENS) for fruitful discussions.

References

- [1] G. Josse, P. Sergot, M. Dorget, and C. Creton, *J. Adhes.*, 2004, **80**, pp 87-118.
- [2] P.G. Saffman and G.I. Taylor, *Proc. Roy. Soc. A*, 1958, **245**, pp 312-329.
- [3] L. Paterson, *J. Fluid Mech.*, 1981, **113**, pp 513-529.
- [4] A. Ghatak and M.K. Chaudhury, *Langmuir*, 2003, **19**, pp2621-2631.
- [5] M. Adda-Bedia and L. Mahadevan, *Proc. R. Soc. A*, 2006, **462**, pp 3233-3251.